CORNERSTONE
♨ MINNESOTA STATE UNIVERSITY MANKATO

Minnesota State University, Mankato
Cornerstone: A Collection of Scholarly and Creative Works for Minnesota State University, Mankato

All Theses, Dissertations, and Other Capstone Projects

Theses, Dissertations, and Other Capstone Projects

2017

Designing a Luminescence Assay to Measure In Vitro Binding of the Fibronectin Attachment Protein (FAP) of Mycobacterium avium subspecies paratuberculosis to Fibronectin

Sirri Ngwa
Minnesota State University, Mankato

Follow this and additional works at: https://cornerstone.lib.mnsu.edu/etds

Part of the Biology Commons, and the Microbiology Commons

Recommended Citation

Designing a Luminescence Assay to Measure *In Vitro* Binding of the Fibronectin Attachment Protein (FAP) of *Mycobacterium avium* subspecies *paratuberculosis* to Fibronectin

By Sirri Ngwa

Advised by Dr. Timothy E. Secott

A Thesis Submitted in Partial Fulfillment of the Requirements for the Degree of

Master of Science

in the

Department of Biological Sciences

Minnesota State University, Mankato

Mankato, Minnesota

December 2017

November 30, 2017

Designing a Luminescence Assay to Measure *In Vitro* Binding of the Fibronectin Attachment Protein (FAP) of *Mycobacterium avium* subspecies *paratuberculosis* to Fibronectin

Sirri Ngwa

This thesis has been examined and approved by the following members of the student's committee.

<u>Dr. Timothy E. Secott</u>
Advisor

<u>Dr. Allison M. Land</u>
Committee Member

<u>Dr. Robert E. Sorensen</u>
Committee Member

Acknowledgements

I want to thank God for giving me the courage to continue my studies after not completing medical school. It has been a long and not so easy journey. I want to thank Minnesota State University, Mankato, Department of Biological Sciences for providing me the opportunity to attend this institution, to serve as a teaching assistant and to conduct research. My gratitude goes especially to Dr. Timothy Secott whose guidance and patience led me to this point. To my committee members, Dr. Allison Land and Dr. Robert Sorensen, your support of my research has been reassuring. Thank you.

To my parents, Samuel and Jemila who have encouraged me to forge ahead when things were tough; and, who offered constructive and spiritual advices, I am immensely grateful for being your daughter! I'm also thankful for my older brothers, Fru, Taiwo, Kehinde and friends who've been my support system. I will like to dedicate my research to my late maternal and paternal grandparents who would have been so proud of my work if they were still on this earth to witness it.

Designing a Luminescence Assay to Measure *In Vitro* Binding of the Fibronectin Attachment Protein (FAP) of Mycobacterium avium subspecies paratuberculosis to Fibronectin

Sirri Ngwa
Master of Science in Biology
Department of Biological Sciences, Minnesota State University, Mankato, Mankato, MN
2017

Abstract

The attachment and penetration of epithelial cells by *Mycobacterium avium* subsp. *paratuberculosis* (MAP) requires a bacterial fibronectin (FN) attachment protein FAP-P, which facilitates binding of FN by MAP. The region of FAP-P that interacts with FN is known, however, the region of FN that is bound by FAP-P is to be determined. Identification of the region of FN to which FAP-P binds would enable the synthesis of a competing peptide that could prevent FN binding by MAP. The first step toward locating this binding site is the design of a reliable FN binding assay. The purpose of this investigation was to determine the optimal conditions (time, temperature, probe concentration, specificity, and color of assay plates) necessary for sensitive, specific binding of FN by FAP-P. Biotinylated peptides representing the FN binding domain of FAP-P and a control peptide were used as probes in a chemiluminescence assay to evaluate the binding of FAP-P to FN. The FAP-P probe bound specifically to FN when probes were incubated for 30 minutes at 37°C in black 96-well microtiter plates. A 10-fold increase in specific FN binding by the FAP-P probe resulted when incubation was increased from 30 minutes to 60 minutes in combination with the use of white microtiter plates over black microtiter plates. A dose dependent binding of FN by the FAP-P probe was observed with increasing probe concentrations (1.0 µg FAP-P, 2.0 µg FAP-P, and 4.0 µg

FAP-P) using optimized conditions. The assay thus described can be used to locate the

FAP-P binding site on FN in protease-generated FN fragments. This, in turn will enable

the design of peptides that could be incorporated into calf management programs that

could block FN binding by MAP and reduce the reduce the incidence of Johne's disease.

Table of Contents

Chapter 1: Literature Review

1.1 Johne's Disease

1.1.1 Overview

Johne's disease is a chronic, usually fatal intestinal disease that primarily affects dairy cattle in the US (1). It is caused by *Mycobacterium avium* subsp. *paratuberculosis* (MAP), which is transmitted by the fecal-oral route (2). The pathogenesis of MAP begins after ingestion and passage through the duodenum, where the organism gets opsonized by fibronectin (FN), a glycoprotein present in bile (3). The MAP-FN complex then travels further down the intestinal tract to the ileum. The epithelial layer of the ileum contains cells known as M cells, which express receptor proteins known as integrins. Integrin receptors bind FN-opsonized MAP and mediate phagocytosis of MAP by these M cells (4, 5). Although there are several FN binding proteins expressed by MAP, the FN attachment protein (FAP) has been shown to be critical for attachment and penetration of M cells by MAP. These M cells convey MAP to macrophages. Once inside a macrophage, MAP inhibits fusion of the phagosome with the lysosomes. This enables MAP to persist and replicate within phagocytic cells (2).

MAP is a very slow-growing organism, so the progression of this disease is likewise very slow (3). It can take two to five years before an infected animal develops clinical disease (1). Diagnostic tests are reliable only when the animals have progressed to the clinical stage of disease. Consequently, Johne's disease results in annual losses of as much as $1 billion to the US cattle industry (6).

The region of FAP to which FN binds has been identified in a closely related subspecies, *Mycobacterium avium* subsp. *hominissuis,* was found to be located within amino acid residues 269-292. The corresponding sequence in FAP-P is identical. However, where the FAP-P peptide binds on FN is not yet known (7). It has been reported that FAP binds to a region near the carboxyl terminus (C-terminus) of the FN monomer, but empirical evidence supporting this conclusion have not yet been published (7).

In this investigation, we propose to optimize the binding between FAP-P and FN in a microplate assay. The successful outcome of this investigation will allow future studies that identify the region of FN that is recognized and bound by FAP-P. This in turn will enable the design of peptides that could be incorporated into calf management programs, which could work by acting as competitors with MAP for FN and reduce the probability of MAP infection. This model could also provide insight into the mechanisms underlying the manifestation of Crohn's disease, a human gastrointestinal inflammatory disease that has been attributed to MAP (8).

1.1.2 History

Johne's disease was first described in 1895 by Johne and Frothingham, who described the presence of acid-fast bacilli in infected cattle intestines. The disease was called pseudo-tuberculous by Bang in 1902, as it was indistinguishable from a form of tuberculosis. By 1908, the disease was reported in the United States, Belgium, Switzerland, Holland, France, Denmark, Germany, and Norway. It wasn't until 1910 that when the disease was called paratuberculosis or Johne's disease, after the causative

organism was isolated by Twort and called *Mycobacterium enteriditis chronicae pseudotuberculosae bovis johne.* Nowadays, Johne's disease has been reported on every continent except Antarctica, threatening the ruminant agriculture worldwide (9)**.**

1.1.3 Economic impact

Johne's disease, or paratuberculosis, is a serious burden on the world dairy industry (9, 10)**.** Economic losses in the dairy industry from paratuberculosis is a result of reduced milk production, premature culling and body-weight losses in cattle slaughter (11). In US dairies, financial losses associated with MAP occurs across all herd sizes and regions. Lost milk production and higher net cow-replacement costs contributed to decreased value of production per cow inventory in herds with Johne's disease (11). When economic losses became substantial, farmers with paratuberculosis-positive herds were encouraged to participate in Johne's disease control programs and farmers with paratuberculosis-negative herds were motivated to devise biosecurity programs to keep MAP from entering their herds (11). In the US dairy industry, Johne's disease is estimated to cost US$22 to US$27 per cow annually in lost revenue and increase cow replacement costs (11).

1.1.4 Stages and symptoms

Johne's disease is characterized as a chronic, granulomatous enteritis caused by ingestion of food, water, milk, or colostrum, contaminated with MAP (1). Infected animals progress through three stages: asymptomatic, clinical, and advanced clinical stages (12). Initial infection of cattle usually occurs within the first weeks of life. Although signs are not typically observed before 2 years of age, younger cattle may shed

viable MAP cells in feces. The clinical stage falls in a period of 2 to 10 years old. At this stage, infected cattle experience poor nutrient absorption, weight loss, increased thirst, and poor milk production (6). Pathology of the small intestine demonstrates that at this stage, the intestinal wall becomes thickened and tissue changes is characterized by the formation of submucosal granulomas (1). If not culled from the herd, cattle progress into an advanced clinical stage where they present with diarrhea, and a general wasting syndrome in which they become anemic, lethargic, emaciated, and too weak to stand (1, 12).

1.2 Management of Johne's disease

Diagnosis of Johne's disease involves detection of MAP, the causative agent, or the identification of an immunological response against MAP. A combination of diagnostic tests and quantitative interpretation of test results provide vital tools for diagnosing Johne's disease. Diagnostic tests helpful in diagnosing Johne's disease include fecal smears, fecal and tissue culture, and enzyme-linked immunosorbent assay (ELISA) (9).

1.2.1 Culture

The gold standard for primary isolation of mycobacteria requires a combination of solid and liquid media with a recommended minimum turnaround time of about 12 weeks after specimen collection to identify mycobacterial species. Meeting these requirements of culture test systems have proven challenging. In addition, the stage of the disease at the time of specimen collection can influence the sensitivity to detect MAP in fecal culture. To culture using a solid media, the standard media used is the Herrold's egg yolk

media (HEY) containing mycobactin J (MJ) (HEYMJ) (13). Colonies become detectable 4-16 weeks after inoculation on the solid medium and may require a subculture step for conclusive identification (13). Utilizing liquid media is faster and more sensitive but the methodology is arduous as scientists must visually inspect culture vials as they handle the samples (14). Successful detection and culture of MAP from animal tissues, milk, breast milk and gut tissues of Crohn's disease patients have been accomplished using the nonradiometric BACTEC Mycobacteria Growth Indicator Tube (MGIT) 960 system (15).

Nevertheless, accurate diagnosis of paratuberculosis is dependent on the long incubation period of the organism (16). Cattle are known to be most susceptible to MAP infections between 0-4 months (16). Clinical disease is most frequently observed in cattle 2-5 years of age (16). A T helper type 1 (T_H1) dominated response controls MAP and viable cells can still be shed in small numbers, which may result in a positive fecal culture test result. Later during infection, the T helper type 2 (T_H2) response as indicated by the presence of anti-MAP antibodies in serum predominates (16). The variation of time in bacterial shedding and antibody responses is speculated to be a result of the variation of infective dose with MAP infections and thus, results in variation in time of the occurrence of positive fecal culture test and positive ELISA tests (16). For accurate MAP diagnosis, scientists should consider the stage of infection of MAP (16). For example, in using an antibody ELISA, the probability of detecting infected cows 2 years of age has been estimated to be 0.06 while the same probability for cows 5 years of age was 0.50 (16, 17).

1.3 Link to Crohn's disease

Crohn's disease (CD) is a chronic inflammatory gastrointestinal tract disease in humans with similar pathological changes and symptoms as Johne's disease in cattle, however, with unknown etiology (18–21). Along with ulcerative colitis, they are both classified as idiopathic inflammatory bowel diseases (IBDs) (20). In western countries, both IBDs display a prevalence of about 150-200 cases per 100,000 persons (20). Previous studies have identified CD as a disorder in genetically predisposed hosts resulting from the effects of environmental factors (20). In the search for IBD-susceptibility genes, genomic investigations have identified several loci for CD in the pericentromeric region of chromosome 16 (identified as *IBD1*) (20).

In 1913, Dalziel reported similarities of CD, Johne's disease, and intestinal tuberculosis (22). Because of this, much attention since then has been focused on a mycobacterial cause of CD, specifically MAP (18, 21). Some data suggest that MAP survives during pasteurization of contaminated milk and dairy products and may pass onto humans during consumption (23–25). However, in recent years, the notion that the causative agent of CD is MAP has been inconsistent (19, 21). The fastidious nature and slow-growing characteristics of MAP have made it challenging to culture and identify the organism from CD patients (18, 21). Differences in microbiological methodologies have also made it difficult to identify MAP (18, 21). In the past, MAP DNA and viable MAP have not been differentiated by polymerase chain reaction (PCR) (21). However, with improved technology and methodologies, researchers have been able to differentiate MAP by PCR by amplifying the insertion sequence of IS*900*; however, this has not

resolved the controversy (18), as several groups have produced conflicting results using PCR. Some have identified MAP by PCR only from some CD patients, whereas other have found MAP PCR products in all patient populations including controls. These differences may be due to differences in the source of MAP, as this organism can be cultured from peripheral blood from patients with CD, breastmilk, and intestinal lymph nodes (21). The possibility also exits that some of these results may have arisen from PCR contamination.

1.4 *Mycobacterium avium* subspecies *paratuberculosis (MAP)*

1.4.1 Classification

The genus *Mycobacterium* belongs to the group Mycobacteria which are Gram positive microorganisms with high GC content (3). They are characterized as a small (0.5×1.5 micron), aerobic, acid-fast, lipid-rich cell wall, bacillus (3, 9). These bacilli are arranged in clumps intertwined by intercellular filaments (9). On artificial media, MAP can be observed as small, glistening, white, rough-smooth colonies (9). Some strains isolated from sheep have been reported to express orange and yellow pigments (9). In addition, lightly-acid-fast and non-acid-fast strains have been observed, which fail to absorb the Ziehl-Neelsen stain. Most can be considered saprophytic; however, they can cause opportunistic infections in immunocompromised persons such as respiratory infections. The growth rate of *Mycobacterium* species correlated loosely with their pathogenic potential. Non-pathogenic members obtain a faster growth rate, whereas pathogenic members obtain a slower growth with generation times nearing 24 hours (3).

The main pathogens of this genus include *Mycobacterium tuberculosis, Mycobacterium leprae, Mycobacterium bovis* and the *Mycobacterium avium* complex (MAC). Members of the MAC are classified as acid-fast, slow-growing bacilli that produce a yellow pigment in the absence of light exposure. They are also opportunistic pathogens known to cause diseases in animals and humans in addition to Crohn's disease (26). Brennan et al demonstrated that the MAC serotype antigens have a common lipopeptidyl-*O*-methyl rhamnose linked to an oligosaccharide; serologic specificity was granted by the specific oligosaccharide residues of the C-mycoside glycopeptidolipids (GLPs), integral constituents of the cell wall and envelope (26, 27). In the past, the MAC included *Mycobacterium avium, Mycobacterium intracellulare* and *Mycobacterium scrofulaceum* forming a serological complex of 31 serotypes of the three species (26). However, current literature does not include *M. scrofulaceum* in the complex due improvements in mycobacterial systematics and the distinction between *M. avium* and *M. intracellulare* (26). Based on nucleic acid studies and phenotypic characteristics, Thorel et al, proposed three subspecies of *M.* avium which include *M. avium* subsp. *avium*, *M. avium* subsp. *paratuberculosis* and *M. avium* subsp. *silvaticum* (28).

Mycobacterium *avium* subspecies *paratuberculosis* (MAP*)* is the causative agent of Johne's disease in ruminants and has also been linked to Crohn's disease in humans. MAP is classified by its generation time, which ranges from 12 hours-24 hours and requires mycobactin, a siderophore (an iron-chelating agent produced by microorganisms) for growth in culture (3, 9).

1.4.2 Genome

In collaboration, the National Animal Disease Center (NADC) and the University of Minnesota have sequenced the MAP genome (3, 29). MAP K-10, the sequenced strain, was obtained from a cow with Johne's disease (3). When MAP K-10 was infected by phage, transformation with plasmid DNA occurred with higher efficiency than that of uninfected MAP K-10 (3).

MAP isolates can be broadly classified into two host-associated types based on their genome analysis and culture characteristic (15, 30): cattle isolates (called C type or Type II) and sheep isolates (called S type or Type I). Both strains are highly similar genetically, and therefore difficult to distinguish (15) Researchers have discovered a third strain called Type III or intermediate, which is a subtype of Type I isolates. Using the IS*1311* insertion sequence, a single nucleotide polymorphism analysis has differentiated three strain types: S, C, and B (also known as Type III); however, this analysis cannot distinguish between Type I and Type III (15). Even though there is a host preference for type S, C or B strains, MAP strains have been observed to cross species and can be isolated from a wide range of animal species including non-ruminants (15). Since the publication of the complete annotated genome sequence of bovine isolate MAP K-10, additional MAP isolates have been sequenced. Results suggest that the bovine isolate MAP K-10 and human isolates are more similar as they contain deletions in the open reading frames (ORFs) MAP1432 through MAP1438c, whereas the sheep isolates do not (15).

1.4.3 Immunology of MAP

In the asymptomatic and subclinical phases of Johne's disease, MAP-infected cattle develop pro-inflammatory and cytotoxic immune responses associated with Type 1 helper T cells (T_H1) (31). This T_H1 immune response is replaced by the Type 2 helper T cells (T_H2)/humoral immune response as the disease advances into the clinical stages (31). At this stage, infected macrophages can be observed within MAP-infected tissues causing extensive inflammation due to the production of IL-1 (31).

In the ileum of MAP infected cattle, severe lesions demonstrated T_H2 predominance and a decrease in regulatory T cells (T_{reg}) gene (FOXP3) expression as compared to healthy cows (31). In contrast, mild ileal lesions display increased $T_H1$responses, and T_{reg} gene expression (31). Conversely, in the mesenteric lymph nodes, expression of FOXP3 is increased with increased lesion severity (31). Within ileal lesions, the change in cytokine profile due to MAP infection leads to a shift in T helper response from T_H1 to T_H2. MAP infection can no longer be controlled, as the anti-MAP antibodies produced (resulting from the switch from T_H1 to T_H2) are ineffective against intracellular MAP. This leads to the development of clinical Johne's disease (31).

In the peripheral blood mononuclear cells (PBMCs), intestinal lesions, and mesenteric lymph nodes of MAP-infected cattle, proinflammatory cytokine gene expression has shown to be altered relative to uninfected cattle (32). PBMCs from sub-clinically infected cattle were seen to have increased expression of IL-10 (32). In MAP-infected ileal tissue, expression of IFN-γ, TGF-β, IL-5, and IL-8 genes was greater and IL-16 expression was lower than in the same tissues in uninfected cattle (32). MAP

infected mesenteric lymph node draining sites demonstrated increased IL-1α, IL-8, IL-2 and IL-10 gene expression whereas TGF-β and IL-16 gene expression was lower (32).

M cells are known as an avenue for antigen access in the initiation of protective immunity. Research has shown that they are capable of engulfing particles from the intestinal lumen to transport them through the epithelial layer into lymphoid tissue (33). MAP has been observed to enter the intestine through M cells located in the epithelium covering Peyer's patches in the ileum of ruminants (7). The continuous Peyer's patch in bovine ileum is a primary lymphoid tissue where B cells develop (33, 34). However, in the bovine upper jejunum are discrete Peyer's patches that are secondary lymphoid tissue that provide adaptive immunity after antigen exposure (33).

Interactions between FAP and FN have been shown to be crucial in the attachment and internalization of MAP, *M. bovis* BCG and *M. leprae* to epithelial cells, *in vitro* (7). The host cell receptors for FN-opsonized mycobacteria *in vitro* have been identified as β1 integrins. M cells display β1 integrins at high density on their luminal surface, making them unique amongst cells of the intestinal epithelium. Thus, the interaction between cell surface integrins and FN bound by organisms may explain why M cells are the portals of entry for MAP (7). Research suggests that bovine ileal M cells take up MAP cells and expel them into the sub/intraepithelial portion of Peyer's patch where they're phagocytosed by macrophages (33). Once in the phagocyte, MAP have been observed to evade host immune response by preventing phagosome-lysosome fusion and allowing MAP to survive and proliferate within macrophages.

1.4.4 Survival

MAP can survive outside the host for long periods and as such can live on and spread in grassland environments (35). It requires about 6 months to a year to eradicate MAP from pasture after infection (35). Published data from an experiment conducted on livestock in the northern hemisphere have demonstrated that MAP cells remain viable in the environment over a long time except in silage (grass compacted and stored in airtight compartments) with low pH or high ammonia levels or in animal house slurry (semiliquid mixture of manure) with urine present (35).

1.4.5 Host species

Although observed as a disease in domestic cattle, sheep, and goats, all ruminants have fallen victim to Johne's disease as illustrated in Table 1.1 (9, 15). In addition, wildlife, and exotic ruminants (deer and boar) and non-ruminants such as fox, crow, wood mouse, badger, rabbit have been recognized to be infected with MAP (12). Monogastric organisms have been observed to be infected with MAP under experimental circumstances (9). Through the use of heavy inocula, horses, chickens, and hogs can be infected; however, the development of clinical disease does not follow (9). Rats, mice, chickens, chicken embryos, pigeons, guinea pigs, hamsters, cats, and rabbits have been used as experimental models to demonstrate aspects of MAP pathobiology such as attachment and invasion of epithelial tissues (9).

Table 1.1: Domestic and wild animals observed to be infected with MAP, either natural, experimental or both.

HOST	DOMESTIC (D) OR WILD (W)	REFERENCES	NATURAL (N), EXPERIMENTAL (E) OR BOTH (B)
Cattle	D	(15, 30)	B
Sheep	D	(15, 30)	B
Goats	D	(15, 30)	B
Red Deer	W	(15, 30, 66, 67)	N
Fallow Deer	W	(15, 30)	B
Bison	W	(15, 30)	N
Wild Boar	W	(15, 30)	N
White Rabbits	W	(66, 67)	N
White-Tailed Deer	W	(66, 67)	N
Exotic Deer	W	(66, 67)	N
Tule Elk	W	(66, 67)	N
Bighorn Sheep	W	(66, 67)	N
Roe Deer	W	(66, 67)	N

1.5 Fibronectin Attachment Protein (FAP)

Fibronectin attachment proteins (FAPs) are a family of homologous fibronectin (FN)-binding glycoproteins that are expressed by several mycobacteria (5, 7, 36–38). Previous research has identified FAPs from different mycobacteria species using polyclonal antibodies to a 50 kDa purified *Mycobacterium vaccae* FAP (FAP-V) (5, 38, 39). These FAPs include *Mycobacterium leprae* (FAP-L), *Mycobacterium avium* (FAP-A), *Mycobacterium bovis* BCG (FAP-B) and *Mycobacterium smegmatis* (FAP-S) (38). FAPs have been shown to be exposed on the bacterial cell surface of *Mycobacterium avium* complex (MAC) and *Mycobacterium tuberculosis* (5, 38, 40–42).The recognized FAPs have been cloned and characterized (38). Two non-contiguous FN binding regions

(amino acids 177-201 (FAP-A-(177-201)) and amino acids 269-292 (FAP-A-(269-292)))
were observed to possess highly conserved FN binding activity using recombinant FAP-
A and FAP-A peptides (5, 38). With the exception of FAP-S, both amino acid sequences
are highly conserved among all identified FAP proteins (5, 38).

Through *in vivo* and *ex vivo* studies, Middleton et al and Zhao et al determined
that the attachment of *Mycobacterium bovis* BCG and *Mycobacterium avium* subsp.
avium to tissues was reliant on the expression of FAP (37, 40, 43). Furthermore, Kuroda
et al, and Schorey et al, proved that cultured epithelial cells were able to endocytose
Mycobacterium bovis BCG and *Mycobacterium leprae* in a FAP dependent method (37,
39, 44).

The region of FAP that is required for FN binding by FAP-A-(amino acid
residues 269-292), has been shown to block the attachment of all mycobacteria tested (*M.
bovis* BCG, *M. smegmatis,* and *M. avium*) to FN-coated surfaces and to evade FN-
opsonized mycobacterial attachment to Schwann cells and epithelial cells in *in vitro*
studies (5, 38). Zhao et al used alanine substitutions in synthetic FAP-A peptides as well
as site-directed mutagenesis of recombinant FAP-A protein to identify a four amino acid
sequence in FAP-A-(269-292), arginine-tryptophan-phenylalanine-valine (RWFV)
necessary for FAP dependent fibronectin binding (38).

MAP possesses a FAP, designated FAP-P, which mediates soluble FN binding (7, 37).

Unlike the other mycobacterial FAPs, FAP-P is not on the surface of MAP; thus, the way

FAP-P interacts with FN may isolate the cell binding domain from host cell receptors.

Secott et al determined that the attachment and endocytosis of MAP by epithelial cells are

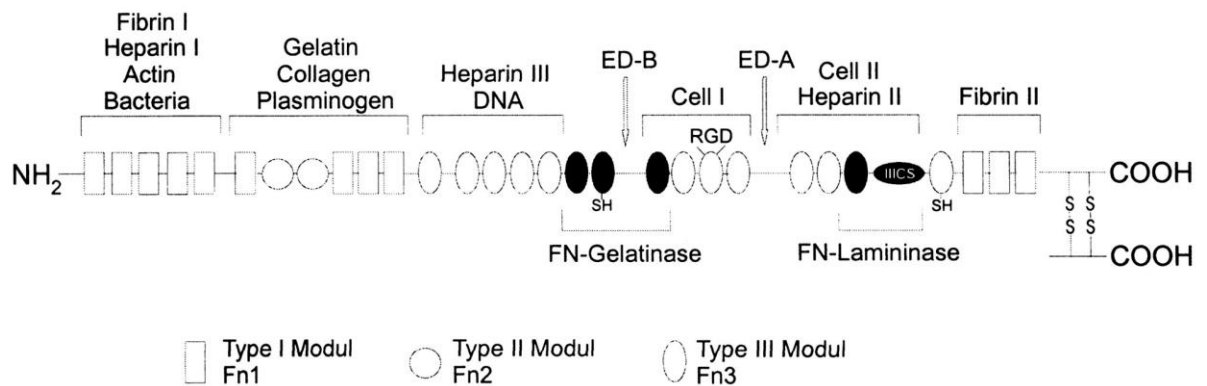FN-dependent processes (37).

1.6 Fibronectin

Figure 1.2: Model of the structure of fibronectin based on a previous study (48). This model shows the internally homologous modules termed type I, II and II. Fibronectin binding domains are indicated at the top of the image.

Fibronectin (FN) is a 420-kDa glycoprotein that is extensively distributed in

mammals (3, 45, 46). Based on amino acid sequence homology, FN is constituted from

repeating structural units designated type I, type II, and type III modules as depicted in

Figure 1.2. Each module is numbered from the N-terminus of FN and contains several

functional domains (46). Fibronectin is found in bodily fluids such as cerebrospinal fluid,

plasma and amniotic fluid as a soluble dimer protomer that consists of two subunits

15

bound by disulfide bridges at the C-termini, and as a polymeric fibrillar network (insoluble form) in the extracellular matrix (ECM) and basement membrane (45, 47).

Fibronectin is a ligand for many cell types such as phagocytic cells and epithelial cells, and is known to interact with macromolecules such as integrins, collagen, fibrin, heparin, actin, gelatin, and complement protein 1 (C1q), sphingolipids, and DNA by integrin surface receptors (3, 45–48). Integrins are known to be involved in cell-cell and cell-extracellular matrix interactions (45).

Fibronectin and integrin interactions are involved in several biological processes such phagocytosis, metastasis, tumor formation, wound healing, lymphocyte recirculation, host cell activation, host cell migration, and microbial pathogenesis (45, 46, 48).

Previous research has demonstrated that whole FN molecules may sometimes have different biological functions than FN fragments (48). Experimentally defined FN fragments were confirmed to be involved in increasing the expression of tumor necrosis factor α, collagenase, TIMP-1, urokinase-type plasminogen activator and stromelysin (49–51). Some fragments established potent inhibition of endothelial cell growth and transformation-promoting activity (52, 53). Native FN, however, did not possess the above functions (48).

At the beginning of an infection, the ability of a bacteria to bind FN-coated surfaces is an important mechanism for the early stage of invasion and colonization of host tissues (47). In a previous study, it was demonstrated that *in vitro* binding of *M. bovis* (BCG) to FN-coated surfaces occurred in a dose-dependent manner with purified

fibronectin (54). As such, we sought to determine a dose effect of our test peptide to FN-coated wells instead of using intact organisms as mentioned above.

1.7 Goal/Rationale

The goal of this project was to optimize the *in vitro* binding of FAP-P to FN under several conditions (time, temperature, probe concentrations, type of microtiter 96-well plate and type of coating protein) to enable the identification of the region of FN recognized by FAP-P.

Chapter 2: Materials and methods

2.1 Reagents, substrates, peptides, and ligands

$NaHCO_3$, Na_2HPO_4, and $C_2H_3O_2$ were purchased from VWR AMRESCO Life Sciences (Solon, OH). NaH_2PO_4 H_2O was purchased from Mallinckrodt Chemical Works (St. Louis, MO). NaCl was purchased from Thermo Fisher (Waltham, MA). Tween 20 was purchased from Thermo Fisher (Waltham, MA). Neutravidin-horseradish peroxidase (HRP) was purchased from Thermo Fisher (Waltham, MA). SuperSignal ELISA Pico chemiluminescent substrate was purchased from Thermo Fisher (Waltham, MA). Ninety-six well Microfluor 1 black and white plates were purchased from Greiner Bio-One North America, Inc. (Monroe, NC). The microplate luminometer (Fluoroskan Ascent FL) was obtained from Thermo Fisher (Waltham, MA). FAP-P (GNRQRWFV) corresponding to amino acid positions 269-276 of FAP-A; and control peptide (GVIGSANA) were used as test and control peptides, respectively (5). These peptides were synthesized and labelled with biotin at the N-terminus by GenScript (Piscataway, NJ). Bovine fibronectin (FN)

was obtained from Alfa Aesar (Ward Hill, MA) and bovine serum albumin (BSA) was

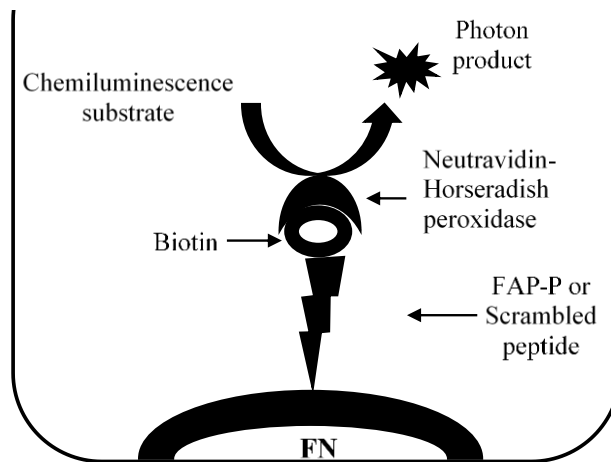obtained from VWR AMRESCO Life Sciences (Solon, OH).

Figure 2.1: Enzyme-linked FN binding assay scheme

2.2 Enzyme-linked FN binding assay

This assay was performed as depicted in Figure 2.1. A 96-well microtiter plate was

coated with intact FN. Bovine serum albumin (BSA) was added to all wells to prevent

non-specific binding. Plates were washed three times with PBST using a squirt bottle.

Biotinylated FAP-P and biotinylated control peptides diluted in ANT buffer and BSA

(control) were added to the appropriate wells and allowed to interact with FN (5).

Fibronectin binding was detected by incubating the FN-coated wells with horseradish

peroxidase (HRP) conjugated to Neutravidin (Thermo Fisher, Chicago, IL). After

washing the plates as described above, the wells were incubated with SuperSignal Pico

(Thermo Fisher), a chemiluminescent substrate for HRP-Neutravidin, for five minutes at room temperature as per manufacturer recommendation. Binding was detected using a microplate luminometer (Thermo Fisher) (5). Each probe was assayed in eight replicates in each of the three independent trials.

To describe the environment in which the interaction of FAP-P to FN in Johne's disease manifests, the FN-binding assay was evaluated under the following parameters:

1. **Temperature effect on FN binding:** the assay was performed at 37°C using ANT buffer (pH 6) as a peptide diluent and at room temperature (25°C) using PBST (pH 7.4) as a peptide diluent.

2. **Time effect on FN binding:** FAP-P peptide and control peptide (at 0.2 µg/well, and 2.0 µg/well for each probe) were incubated at 30 minutes and 60 minutes in FN-coated wells.

3. **96-well microtiter plate type effect on FN binding:** Black 96-well microtiter plates and white 96-well microtiter plates were used for this luminescent assay to determine which plate obtains the best/higher signal-to-noise ratio.

4. **Specificity of FN binding:** The assay was performed with half the microtiter plate coated with FN alone and the other half of the microtiter plate coated with BSA alone to determine if the FAP-P probe binds to FN only or to any readily available protein.

5. **Probe (FAP-P) concentration effect on FN binding:** To determine if a dose effect existed between the FAP-P probe and FN, concentrations of 0.2 µg, 1.0 µg,

2.0 µg, and 4.0 µg of each probe were added to individual FN-coated wells and

incubated at 37°C for 60 minutes.

2.3 Statistics

The statistical analyses Kruskal-Wallis H test, post hoc test and Student's unpaired t

test were performed using GraphPad Prism 4.

Chapter 3: Results

3.1 Specificity of FN binding

BSA and all probes were incubated for 30 minutes at 37 °C in both FN-coated and

BSA-coated wells. Luminescent signal from FN-coated wells probed with 2.0 µg FAP-P

peptide was significantly greater than those probed with BSA and control peptides regardless

of well coating ($P \leq 0.001$) (Fig. 3.1). Each probe appeared to bind to FN-coated wells more

readily than to BSA-coated wells with increasing background signal. Signal from the FAP-P

probe was approximately 4-fold higher for FN-coated wells as compared to those coated with

BSA. This indicates that probe concentration of 2 µg per well may be necessary to reveal

specific binding of the FAP-P peptide to FN.

3.2 Effect of temperature on FN binding

FN binding assays in this investigation were conducted at 25°C and 37°C (Fig. 3.2)

using FN-coated black 96-well microtiter plates with probes incubated for 30 minutes.

Binding of FAP-P probe when used at 2.0 µg per well resulted in significantly higher signal

than that of the control peptide at both 25°C and 37°C. However, the peak signal was greater

at 37°C ($P \leq 0.01$). These observations indicate that attachment of FAP-P to FN may be

influenced by temperature over a short time frame (30 minutes). When FN-coated wells were probed at 25°C and 37°C with 2.0 µg FAP-P peptide were compared directly using Student's T test, the signal to noise ratio at 37°C was nearly twice that observed at 25°C, and this effect was significant ($P = 0.0003$) (Fig 3.3). For this reason, subsequent experiments were conducted at 37°C.

3.3 Effect of microtiter plate type on FN binding

To assess the effects of microtiter plate color on the interaction of FAP-P with FN, the FN binding assay was conducted on both black and white 96-well microtiter plates with probes incubated for 30 minutes (Fig. 3.4).

When incubated in white microtiter plates for 30 minutes, the amount of signal observed was approximately 8-fold higher than black microtiter plates. While FN-coated white microtiter plate wells probed with 2.0 µg FAP-P peptide yielded signal that was significantly higher than all treatments in black plates ($P \leq 0.001$), the signal was not significantly different from those other wells probed with BSA or control peptides on FN-coated white microtiter plates wells except for 2.0 µg control peptide.

When probes were incubated with FN-coated wells using white microtiter plates for 60 minutes (Fig 3.5), wells probed with 2.0 µg FAP-P peptide yielded significantly higher signal than those probed with all other probes ($P \leq 0.001$) except for 2.0 µg FAP-P peptide at 30 minutes. When FN-coated wells were probed at 30 minutes and 60 minutes with 2.0 µg FAP-P peptide were compared directly using Student's *T* test, the signal to noise ratio at 60 minutes was greater than that observed at 30 minutes, and this effect was significant ($P < 0.0001$) (Fig 3.6). The specific signal level was increased approximately 3-fold over that

which was observed at 30 minutes of probing whereas the relative signal decreased. Thus, probing FN with FAP-P peptide for 60 minutes yielded the highest specific signal in white microtiter plates.

3.4 FN binding dose response curve

We next sought to determine if we could increase signal by increasing probe concentrations (Fig. 3.7). Increasing the concentrations of control peptide did not reveal a significant dose effect ($R^2 = 0.04$) (Fig. 3.7). In contrast, the level of signal increased as the concentration of FAP-P peptides increased, to the extent that probe binding could be modeled using a second order polynomial expression ($R^2 = 0.72$) (Fig. 3.7). Thus, the ELBA described herein can be used as a quantitative FN binding assay, as well as the presence or absence of binding.
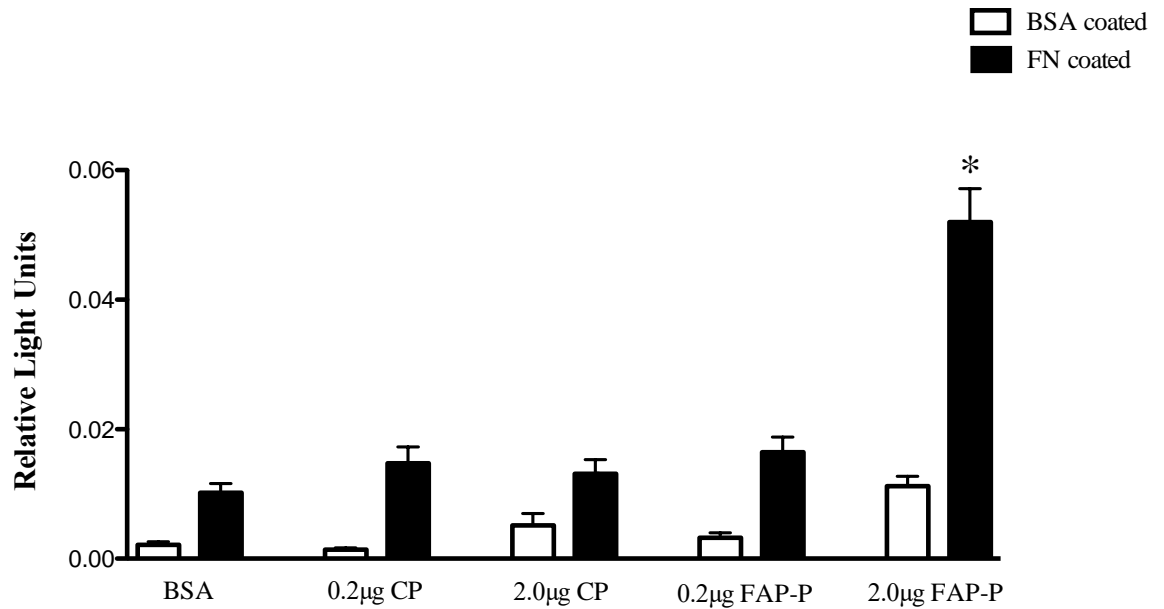
Figure 3.1: Specificity of FN binding. FN binding assay was conducted on a black microtiter 96-well plate. Half the plate was treated with intact FN and the other half was treated with bovine serum albumin (BSA) overnight. Control peptides and FAP-P peptides were incubated at 37°C for 30 minutes in designated wells containing FN or BSA. The asterisk indicates a significant difference ($P \leq 0.001$) between 2.0 µg FAP-P peptide in FN-coated wells and other treatments.
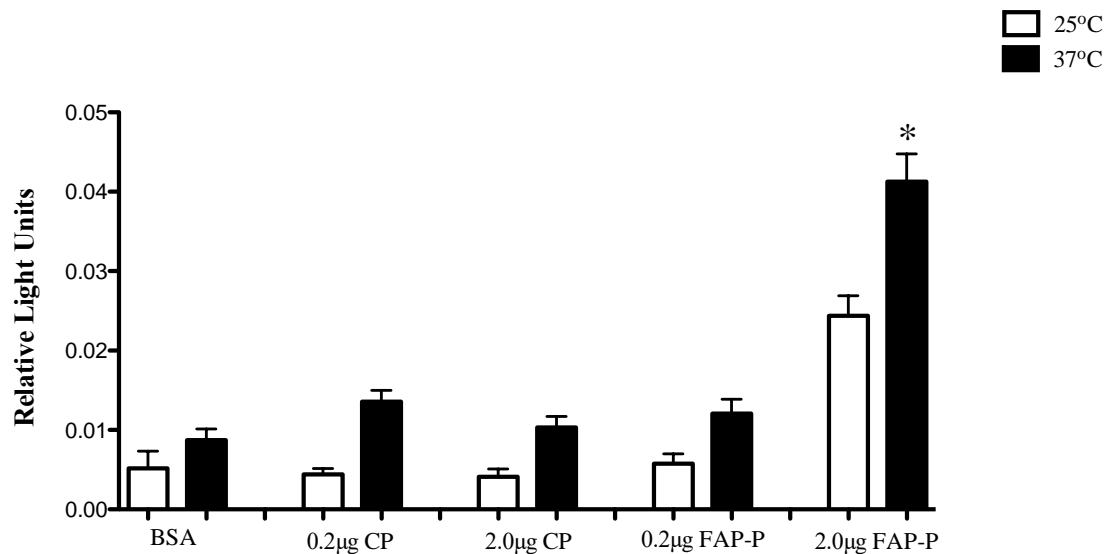
Figure 3.2: Effect of temperature on FN binding. Assays were conducted on a black 96-well microtiter plates. Designated wells were treated with intact FN overnight. Control peptides and FAP-P peptides were incubated at 25ºC or 37ºC for 30 minutes in FN-coated wells. The asterisk indicates a significant difference ($P \leq 0.01$) between 2.0 μg FAP-P peptide at 37ºC and other treatments.
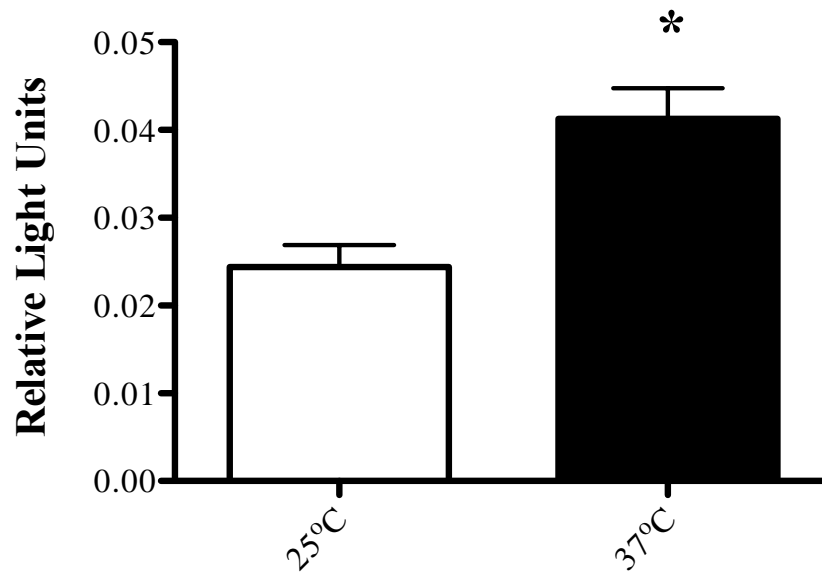
Figure 3.3. Binding of 2.0 μg FAP-P to FN-coated wells at 25°C and 37°C were compared by Student's *T* test. The asterisk indicates a significant difference ($P \leq 0.0003$) between 37°C and 25°C.
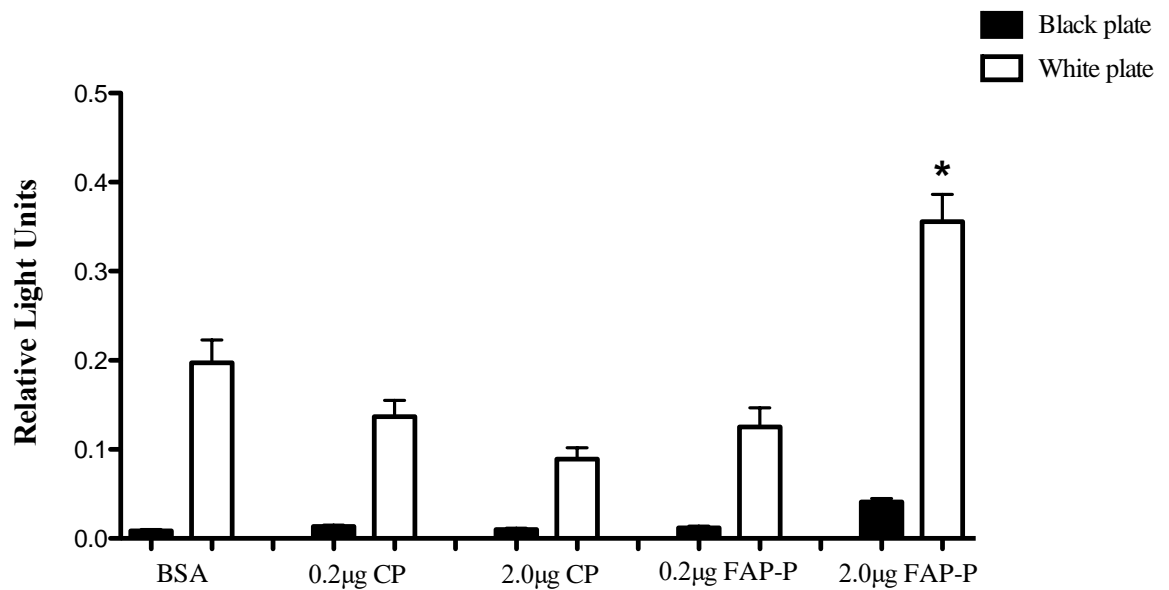
Figure 3.4: Effect of microplate type on FN binding. This assay was conducted on a white 96-well microtiter plate and a black 96-well microtiter plate and treated with intact FN overnight. Control peptides and FAP-P peptides were incubated in in FN-coated wells in either black or white microtiter plates at 37°C for 30 minutes. The asterisk indicates a significant difference ($P \leq 0.001$) between 2.0 μg FAP-P peptide in FN-coated wells in white microtiter plates and other treatments.
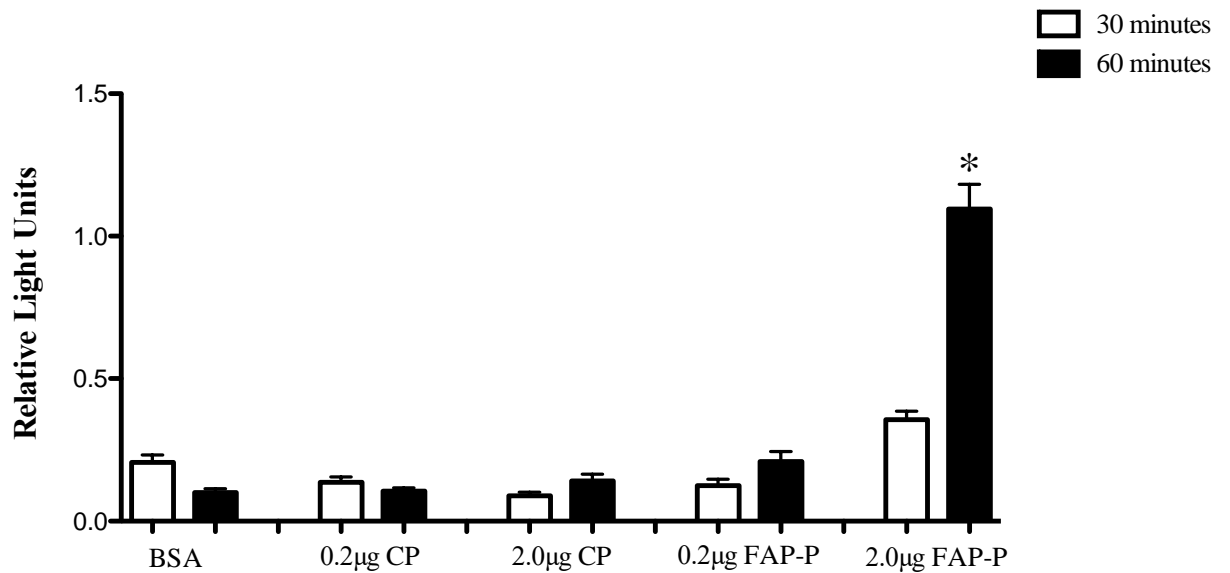
Figure 3.5: Effect of incubation time on FN binding. White 96-well microtiter plates were treated with intact FN overnight. Control peptides and FAP-P peptides were both incubated at 37°C for 30 minutes or 60 minutes in FN-coated wells. An asterisk indicates a significant difference ($P \leq 0.001$) between 2.0 μg FAP-P peptide in FN-coated wells incubated for 60 minutes and other treatments.
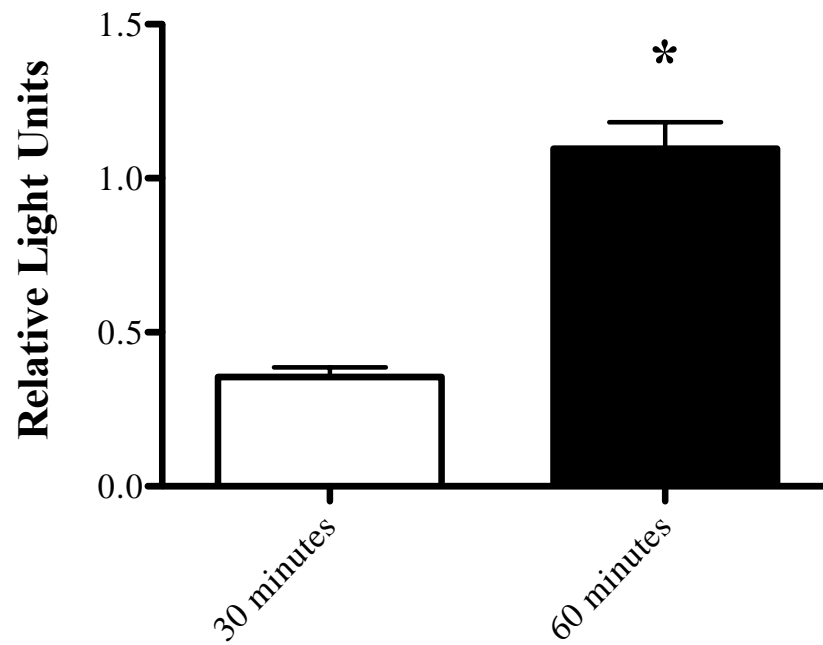
Figure 3.6. Binding of 2.0 µg FAP-P to FN at 30 minutes and 60 minutes incubation were compared by Student's *T* test. The asterisk indicates a significant difference ($P \leq 0.0001$) between 60 minutes and 30 minutes.
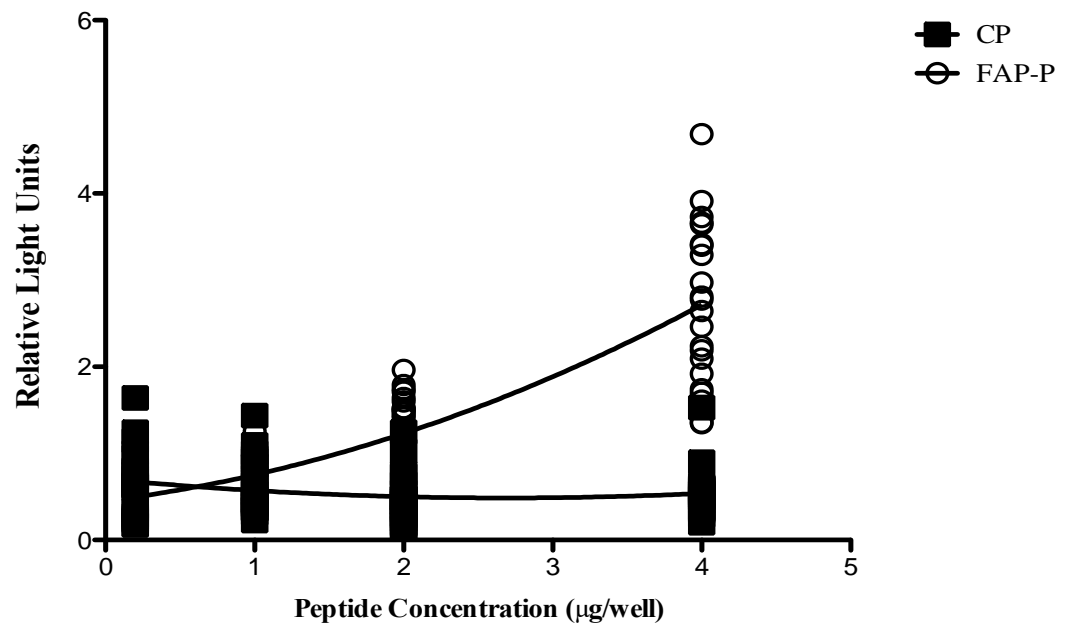
**Figure 3.7:** FAP-P dose response curve on FN binding. Positive conditions of the FN binding assay were used to determine FAP-P dose effect of binding to FN. White 96-well microtiter plates were treated with intact FN overnight. Control peptides (CP) and FAP-P peptides at 0.2 μg, 1.0 μg, 2.0 μg and 4.0 μg were incubated at 37ºC for 60 minutes in FN-coated wells. CP is not significant at $R^2 = 0.04$ and FAP-P is significant at $R^2=0.72$.

Chapter 4: Discussion

The long-term goal of our research plan is to reduce the incidence of Johne's disease. The intermediate goal is to identify the region of FN that is recognized and bound by FAP-P, as this is not yet known (7). To achieve this, it is necessary to develop an effective assay to measure FAP-P binding to FN.

As part of this optimization, we considered specificity of binding, temperature, time, microtiter plate type, and a probe dose response. A previous attempt to develop a colorimetric FN binding assay was hampered by very low signal-to-noise ratios (Breland and Secott, unpublished data). We therefore chose to use chemiluminescence because of the high sensitivity afforded by chemiluminescence detection (55, 56). In this investigation, we confirmed that FAP-P peptide binds specifically to intact FN. Lastly, we determined that by using white microtiter plates we were able to obtain increased FN binding signal as compared to that seen with black microtiter plates. Furthermore, we observed greater binding when probes were incubated at 37ºC for 60 minutes. In addition, we were able to demonstrate that binding of FN by FAP-P increases with increased concentration of FAP-P peptides. Overall, we produced an enzyme-linked FN binding assay with a high signal-to-noise ratio and high sensitivity.

A previous investigation reported that MAP invades intestinal tissue through the binding of the MAP protein FAP-P to fibronectin (FN). This binding is facilitated by integrins expressed on the luminal surface of M cells. The purpose of this investigation was to take an *in vivo* phenomenon such as FN binding by FAP-P and create an *in vitro* system where this interaction between FAP-P and FN can be more closely examined and

defined. To the best of our knowledge, this investigation is the first of its kind to measure FAP-P binding to FN.

In this investigation, we determined that the FAP-P peptide binds specifically to FN. The apparent background signal for controls does not reflect non-specific probe binding, because the same results were realized with BSA which did not have a biotin label. Thus, the background signal more than likely reflects horseradish peroxidase (HRP)-Neutravidin binding to the ligands other than biotin. In addition, HRP-Neutravidin seemed to have bound FN-coated wells more readily than BSA-coated wells. Neutravidin is known to have fewer non-specific interactions than streptavidin and avidin (57). Avidin has a very high affinity for biotin and as such may bind to other proteins as biotin is found in mammalian cells (57). Streptavidin, on the other hand, has a peptide sequence (RYD) that resembles the binding sequence (RGD) of fibronectin (57). Consequently, this may have led to much of the background signal seen with this assay (57).

Temperature influences the activity of horseradish peroxidase (HRP) (58). An investigation of HRP-antibody conjugate activity showed that the signal reaches its plateau relatively early at 37°C, whereas at 25 $^\circ$C, the HRP signal continues to develop for several hours. Nevertheless, signal development occurred at the same rate for both temperatures (58). It is also possible that the higher temperature may have an influence on the conformation of the FAP-P peptide, which resulted in a stronger signal (58).

Additionally, while the FAP-P peptide was positively charged (+2) and the control peptide was neutral (59), background signal was greater for FN-coated wells than for BSA-coated wells regardless of the probe used. At neutral pH (PBST), HRP-

Neutravidin is slightly negative, with an isoelectric point (pI) = 6.3; FN is more negative (pI = 5.5-6) than HRP-Neutravidin and BSA very negatively charged (pI=4.8) (60). The differences in isoelectric points may explain why unspecific binding was observed in FN-coated wells than in BSA-coated wells.

This investigation determined that FN binding to FAP-P peptide was greater at 37°C. This temperature is a commonly used temperature to conduct immunoassays relating to warm-blooded animals. We sought to observe binding of FAP-P to FN at this same temperature and at room temperature (25°C); however, that goal was confounded by a simultaneous change in pH of the peptide diluent buffers we used. At the onset of this investigation, the probes were diluted using PBST (pH 7.4) for the 25°C FN binding assay. However, it has been demonstrated that the binding of FN by MAP is activated by passage through an acidic environment in the ruminant digestive tract (7, 37). Secott, et al. found that FN binding by the intact organism is best observed when the organism is exposed to an acidic environment. As such, we proceeded to conduct our 37°C FN binding assay with probes diluted using ANT buffer (pH 6). Given that assays run at 37°C in ANT buffer produced greater signal, this observation could support the conclusion that *in vitro* binding of FN by FAP-P, is influenced by pH.

However, Secott et al noted that at neutral pH, the crucial FN-binding residues [273]RWFV[276] within the FAP-P peptide have a net positive charge that would be unaltered in an acidic environment (7). Thus, the choice of probing buffer used in this assay may have had little effect on the binding of the probe. As such, what we observed is believed to be a temperature effect rather than a pH effect. Nevertheless, these experiments should

be repeated at 25ºC using ANT buffer-treated probes. While increased temperature would be expected to increase the frequency of intermolecular collisions, it may also have improved the stability of the FN-FAP-P interaction.

We realized higher FN binding signal with white microtiter plates than with black microtiter plates. Black objects tend to absorb all light wavelengths and reflect none, whereas white objects tend to reflect all light wavelengths and absorb none. For luminescence and fluorescence immunoassays, white and black 96-well microtiter plates respectively are usually recommended (61). However, phosphorescence (emission of light by a substance from stored energy) associated with the white microtiter plates can result in higher background signal (62). As a result, the choice of microtiter plate type should be based on experimental evidence. Our findings revealed that the use of white 96-well microtiter plates resulted in a 10-fold increase in FN binding signal by the FAP-P peptide over that seen for black 96-well microtiter plates. Regardless of the plate type used, it is critical that luminescence assays be protected from light and white microtiter plate are more susceptible to light interference (61–64).

For this study, we attempted to increase the signal by increasing probe incubation time. We detected greater binding between FAP-P and FN with increased (60 minutes) probing time as compared to that seen at 30 minutes. The observation that a doubling of the binding time resulted in a nearly 3-fold increase in signal suggests that the FAP-P-FN interaction is not simply a first order reaction. We have not established the time necessary for FAP-P-FN binding to reach equilibrium (65). Additional experiments using longer probing times will be necessary to optimize the timing of this step.

Ratliff et al established that *in vitro* binding of *Mycobacterium bovis* (BCG) to FN-coated surfaces occurred in a dose-dependent manner with purified fibronectin (54). We sought to determine the concentration of test peptide required to detect a positive FN binding response in Johne's disease. Increased FAP-P peptide concentration lead to increased FN binding. We did not manipulate the coating protein concentration. As such, we showed that FAP-P binds to FN in a dose-dependent manner. Therefore, this FN binding assay could be used in a quantitative format. In addition, we have not determined the maximum dose of the FAP-P peptide to bind intact FN. Thus, we need to determine the linear range of this FN binding assay.

One of the difficulties encountered in this investigation involved the source of our soluble fibronectin. The FN solutions used in this investigation were purchased several times from three suppliers. This was due to the protein solution becoming unstable and polymerizing in storage, preventing even distribution into microplate wells. Consequently, the results of our assay varied in earlier trials. The last batch was lyophilized in Tris buffer. After reconstitution in sterile water according to manufacturer instructions, the solution had to be stored for one week at 4°C to be completely dissolved. We then stored this in single use aliquots at -20°C. This approach enabled us to realize more consistent results.

We used synthesized FAP-P peptides to probe FN instead of using intact MAP cells in culture. The reason for avoiding intact MAP was to eliminate problems arising from MAP culture contamination. Further, the use of intact MAP would have meant that MAP-FN interaction would not be limited to FAP-P, as MAP expresses several FN

binding proteins (7). Finally, due to the slow-growing nature of MAP, it would have taken considerably longer to conduct this series of experiments.

The outcome of this investigation will allow for the FN region that is recognized and bound by FAP-P to be identified. To do so, researchers would have to first conduct proteolytic cleavage of FN, purify the FN fragments by electroelution, coat white microtiter plates with purified FN fragments, and finally probe with biotinylated FAP-P peptide to identify the region of FN to which FAP-P binds.

The FN binding assay could be further refined by examining the effects of conjugate concentration on assay signal and specificity. We could also incorporate a second blocking step between probing and addition of conjugate, to further reduce background noise.

Another goal enabled by this research will be to determine if FAP-P recognizes a linear epitope of fibronectin rather than a conformational epitope of fibronectin. This information could lead to the synthesis of a peptide/protein that could be added to colostrum and used as a milk replacer for calves. This synthesized peptide would behave as a FAP-P competitor to minimize binding of MAP to fibronectin.

The data presented in this thesis described the optimization of an assay to detect FN binding using a chemiluminescence probe which will be useful for identifying the binding domain on FN by FAP-P. This is an essential component in the design of a peptide to inhibit MAP binding to bovine intestinal epithelial cells. As such, the results of this investigation will likely lead to a reduction in the incidence of Johne's disease,

increasing the profitability of dairy farming while preserving the supply of safe,

affordable dairy products for the consumers.

References

1.   Arsenault RJ, Maattanen P, Daigle J, Potter A, Griebel P, Napper S. 2014. From

         mouth to macrophage: mechanisms of innate immune subversion by

         Mycobacterium avium subsp. *paratuberculosis*. Vet Res 45:1–15.

2.   McFadden JJ, Butcher PD, Chiodini R, Hermon-Taylor J. 1987. Crohn's disease-

         isolated mycobacteria are identical to *Mycobacterium paratuberculosis*, as

         determined by DNA probes that distinguish between mycobacterial species. J Clin

         Microbiol 25:796–801.

3.   Chacon O, Bermudez LE, Barletta RG. 2004. Johne's disease, inflammatory bowel

         disease, and *Mycobacterium paratuberculosis*. Annu Rev Microbiol 58:329–363.

4.   Johnston CD. 2014. Enhanced expression of codon optimized *Mycobacterium*

         avium subsp. *paratuberculosis* antigens in *Lactobacillus salivarius*. Front Cell

         Infect Microbiol 4:1–11.

5.   Schorey JS, Holsti M a, Ratliff TL, Allen PM, Brown EJ. 1996. Characterization

         of the fibronectin-attachment protein of *Mycobacterium avium* reveals a

         fibronectin-binding motif conserved among mycobacteria. Mol Microbiol 21:321–

         329.

6.   Bannantine JP, Bermudez LE. 2013. No holes barred: Invasion of the intestinal

         mucosa by *Mycobacterium avium* subsp. *paratuberculosis*. Infect Immun 81:3960–

         3965.

7.   Secott TE, Lin TL, Wu CC. 2001. Fibronectin attachment protein homologue mediates fibronectin binding by *Mycobacterium avium* subsp. *paratuberculosis*. Infect Immun 69:2075–2082.

8.   Lee JS, Shin SJ, Collins MT, Jung ID, Jeong Y-I, Lee C-M, Shin YK, Kim D, Park Y-M. 2009. *Mycobacterium avium* subsp. *paratuberculosis* fibronectin attachment protein activates dendritic cells and induces a Th1 polarization. Infect Immun 77:2979–88.

9.   Chiodini RJ, Van Kruiningen HJ, Merkal RS. 1984. Ruminant paratuberculosis (Johne's disease): the current status and future prospects. Cornell Vet 74:218–262.

10.   Bhattarai B, Fosgate GT, Osterstock JB, Fossler CP, Park SC, Roussel AJ. 2013. Perceptions of veterinarians in bovine practice and producers with beef cow-calf operations enrolled in the US voluntary bovine Johne's disease control program concerning economic losses associated with Johne's disease. Prev Vet Med 112:330–337.

11.   Ott SL, Wells SJ, Wagner BA. 1999. Herd-level economic losses associated with Johne's disease on US dairy operations. Prev Vet Med 40:179–192.

12.   Tiwari A, VanLeeuwen JA, McKenna SLB, Keefe GP, Barkema HW. 2006. Johne's disease in Canada Part I: clinical symptoms, pathophysiology, diagnosis, and prevalence in dairy herds. Can Vet J 47:874–82.

13.   Payeur JB. 2005. Current culture methods for *Mycobacterium avium* subspecies

paratuberculosis, p. 352–358. *In* Proceedings of 81CP 2005.

14. Piersimoni C, Scarparo C, Callegaro A, Passerini Tosi C, Nista D, Bornigia S, Scagnelli M, Rigon A, Ruggiero G, Goglio A. 2001. Comparison of MB/BacT ALERT 3D system with radiometric BACTEC system and Löwenstein-Jensen medium for recovery and identification of mycobacteria from clinical specimens: A multicenter Study. J Clin Microbiol 39:651–657.

15. Abendaño N, Sevilla I, Prieto JM, Garrido JM, Juste RA, Alonso-Hearn M. 2012. Quantification of *Mycobacterium avium* subsp. *paratuberculosis* strains representing distinct genotypes and isolated from domestic and wildlife animal species by use of an automatic liquid culture system. J Clin Microbiol 50:2609–2617.

16. Nielsen SS, Toft N. 2008. Ante mortem diagnosis of paratuberculosis: A review of accuracies of ELISA, interferon-γ assay and faecal culture techniques. Vet Microbiol 129:217–235.

17. Nielsen SS, Toft N. 2006. Age-specific characteristics of ELISA and fecal culture for purpose-specific testing for paratuberculosis. J Dairy Sci 89:569–579.

18. Rowbotham DS, Mapstone NP, Trejdosiewicz LK, Howdle PD, Quirke P. 1995. *Mycobacterium paratuberculosis* DNA not detected in Crohn's disease tissue by fluorescent polymerase chain reaction. Gut 37:660–667.

19. Greenstein RJ. 2003. Is Crohn's disease caused by a mycobacterium? Comparisons

with leprosy, tuberculosis, and Johne's disease. Lancet Infect Dis 3:507–514.

20. Ogura Y, Bonen DK, Inohara N, Nicolae DL, Chen FF, Ramos R, Britton H, Moran T, Karaliuskas R, Duerr RH, Achkar JP, Brant SR, Bayless TM, Kirschner BS, Hanauer SB, Nuñez G, Cho JH. 2001. A frameshift mutation in NOD2 associated with susceptibility to Crohn's disease. Nature 411:603–606.

21. Naser SA, Ghobrial G, Romero C, Valentine JF. 2004. Culture of *Mycobacterium avium* subspecies *paratuberculosis* from the blood of patients with Crohn's disease. Lancet 364:1039–1044.

22. Dalziel TK. 1913. Chronic interstitial enteritis. Br Med J 2:1068–1070.

23. Tasara T, Stephan R. 2005. Development of an F57 sequence-based real-time PCR assay for detection of *Mycobacterium avium* subsp. *paratuberculosis* in milk. Appl Environ Microbiol 71:5957–5968.

24. Grant IR, Rowe MT. 2004. Effect of chemical decontamination and refrigerated storage on the isolation of *Mycobacterium avium* subsp. *paratuberculosis* from heat-treated milk. Lett Appl Microbiol 38:283–288.

25. Slana I, Liapi M, Moravkova M, Kralova A, Pavlik I. 2009. *Mycobacterium avium* subsp. *paratuberculosis* in cow bulk tank milk in Cyprus detected by culture and quantitative IS*900* and F57 real-time PCR. Prev Vet Med 89:223–226.

26. Inderlied CB, Kemper CA, Bermudez LE. 1993. The *Mycobacterium avium* complex. Clin Microbiol Rev 6:266–310.

27. Brennan PJ, Aspinall GO, Nam Shin JE. 1981. Structure of the specific oligosaccharides from the glycopeptidolipid antigens of serovars in the *Mycobacterium avium-Mycobacterium intracellulare-Mycobacterium scrofulaceum* complex. J Biol Chem 256:6817–6822.

28. Thorel, M, Krichevsky, M, Vincent Levy-Frebault V. 1990. Numerical taxonomy of mycobactin-dependent mycobacteria, emended description of *Mycobacterium avium*, and description of *Mycobacterium avium* subsp. *avium* subsp. *nov*., *Mycobacterium avium* subsp. *paratuberculosis* subsp. *nov*., and *Mycobacterium avium* subsp. *s*. Int J Syst Bacteriol 40:254–260.

29. Paustian ML, Amonsin A, Kapur V, Bannantine JP. 2004. Characterization of novel coding sequences specific to *Mycobacterium avium* subsp. *paratuberculosis*: implications for diagnosis of Johne's disease 42:2675–2681.

30. Abendaño N, Sevilla IA, Prieto JM, Garrido JM, Juste RA, Alonso-Hearn M. 2013. *Mycobacterium avium* subspecies *paratuberculosis* isolates from sheep and goats show reduced persistence in bovine macrophages than cattle, bison, deer and wild boar strains regardless of genotype. Vet Microbiol 163:325–334.

31. Roussey JA, Oliveira LJ, Langohr IM, Sledge DG, Coussens PM. 2016. Regulatory T cells and immune profiling in Johne's disease lesions. Vet Immunol Immunopathol 181:39–50.

32. Coussens P, Verman N, Coussens M, Elftman M, McNulty A. 2004. Cytokine gene expression in peripheral blood mononuclear cells and tissues of cattle

infected with *Mycobacterium avium* subsp. *paratuberculosis*: evidence for an inherent proinflammatory gene expression pattern. Infect Immun 72:1409–1422.

33. Momotani E, Whipple DL, Thiermann a B, Cheville NF. 1988. Role of M cells and macrophages in the entrance of *Mycobacterium paratuberculosis* into domes of ileal Peyer's patches in calves. Vet Pathol 25:131–137.

34. Yasuda M, Jenne CN, Kennedy LJ, Reynolds JD. 2006. The sheep and cattle Peyer's patch as a site of B-cell development. Vet Res 37:401–415.

35. Whittington RJ, Marshall DJ, Nicholls PJ, Marsh IB, Reddacliff LA. 2004. Survival and dormancy of *Mycobacterium avium* subsp. *paratuberculosis* in the environment. Society 70:2989–3004.

36. Secott TE, Lin TL, Wu CC. 2004. *Mycobacterium avium* subsp. *paratuberculosis* fibronectin attachment protein facilitates M-cell targeting and invasion through a fibronectin bridge with host integrins. Infect Immun 72:3724–3732.

37. Secott TE, Lin TL, Wu CC. 2002. Fibronectin attachment protein is necessary for efficient attachment and invasion of epithelial cells by *Mycobacterium avium* subsp. *paratuberculosis*. Infect Immun 70:2670–2675.

38. Zhao W, Schorey JS, Groger R, Allen PM, Brown EJ, Ratliff TL. 1999. Characterization of the fibronectin binding motif for a unique mycobacterial fibronectin attachment protein, FAP. J Biol Chem 274:4521–4526.

39. Schorey JS, Li Q, Court DWMC, Bong-Mastek M, Clark-Curtiss JE, Ratliff TL,

Brown EJ. 1995. A *Mycobacterium leprae* gene encoding a fibronectin binding protein is used for efficient invasion of epithelial cells and schwann cells. 63:2652–2657.

40.   Middleton AM, Chadwick M V., Nicholson AG, Dewar A, Groger RK, Brown EJ, Wilson R. 2000. The role of *Mycobacterium avium* complex fibronectin attachment protein in adherence to the human respiratory mucosa. Mol Microbiol 38:381–391.

41.   Rao SP, Gehlsen KR, Catanzaro A. 1992. Identification of a beta 1 integrin on *Mycobacterium avium-Mycobacterium intracellulare*. Infect Immun 60:3652–3657.

42.   Verbelen C, Dufrêne YF. 2009. Direct measurement of mycobacterium–fibronectin interactions. Integr Biol 1:296.

43.   Zhao W, Schorey JS, Bong-Mastek M, Ritchey J, Brown EJ, Ratliff TL. 2000. Role of a bacillus Calmette-Guérin fibronectin attachment protein in BCG-induced antitumor activity. Int J Cancer 86:83–88.

44.   Kuroda K, Brown EJ, Telle WB, Russell DG, Ratliff TL. 1993. Characterization of the internalization of bacillus Calmette-Guérin by human bladder tumor cells. J Clin Invest 91:69–76.

45.   Johansson S, Svineng G, Wennerberg K, Armulik A, Lohikangas L. 1997. Fibronectin-integrin interactions. Front Biosci 2:d126-46.

46. Naito M, Fukuda T, Sekiguchi K, Yamada T. 2000. The domains of human fibronectin mediating the binding of α antigen, the most immunopotent antigen of mycobacteria that induces protective immunity against mycobacterial infection. Biochem J 731:725–731.

47. Ratliff TL, McGarr J a, Abou-Zeid C, Rook G a, Stanford JL, Aslanzadeh J, Brown EJ. 1988. Attachment of mycobacteria to fibronectin-coated surfaces. J Gen Microbiol 134:1307–1313.

48. Unger J, Tschesche H. 1999. The proteolytic activity and cleavage specificity of fibronectin-gelatinase and fibronectin-lamininase. J Protein Chem 18:403–411.

49. Bewsey KE, Wen C, Purple C, Homandberg GA. 1996. Fibronectin fragments induce the expression of stromelysin-1 mRNA and protein in bovine chondrocytes in monolayer culture. Biochim Biophys Acta 1317:55–64.

50. Xie DL, Hui F, Meyers R, Homandberg GA. 1994. Cartilage chondrolysis by fibronectin fragments is associated with release of several proteinases: stromelysin plays a major role in chondrolysis. Arch Biochem Biophys 311:205–212.

51. Beezhold DH, Personius C. 1992. Fibronectin secretion. J Leukoc Biol 51:59–64.

52. De Petro G, Barlati S, Vartio T, Vaheri A. 1983. Transformation-enhancing activity in plasma of tumor patients: relationship with fibronectin fragments. Int J Cancer 31:157–162.

53. Homandberg GA, Kramer-bjerke J, Grant D. 1986. Heparin-binding fragments of

fibronectin are potent inhibitors of endothelial cell growth: structure-function correlations. Biochim Biophys Acta 874:61–71.

54. Ratliff TL, Palmer JO, Mcgarr JA, Brown EJ. 1987. Intravesical bacillus Calmette-Guérin therapy for murine bladder tumors: initiation of the response by fibronectin-mediated attachment of bacillus Calmette-Guérin 1762–1766.

55. Bronstein I, Martin CS, Fortin JJ, Olesen CEM, Voyta JC. 1996. Chemiluminescence: sensitive detection technology for reporter gene assays. Clin Chem 42:1542–1546.

56. Bouaïcha N, Maatouk I, Vincent G, Levi Y. 2002. A colorimetric and fluorometric microplate assay for the detection of microcystin-LR in drinking water without preconcentration. Food Chem Toxicol 40:1677–1683.

57. Invitrogen. 2009. Avidin and NeutrAvidin™ biotin-binding proteins and conjugates. Mol Probes.

58. Ngo TT, Lenhoff HM. 2012. Enzyme-mediated immunoassay. Springer Science & Business Media; Plenum Press, Irvine, CA.

59. Innovagen. Peptide property calculator. PepCalc.com.

60. Invitrogen by Thermo Fisher Scientific. 2010. Antibodies, avidins and lectins, p. 241–288. *In* The Molecular Probes® Handbook-A Guide to Fluorescent Probes and Labeling Technologies 11th Edition.

61. Hirmann D, Loibner AP, Braun R, Szolar OHJ. 2007. Applicability of the

bioluminescence inhibition test in the 96-well microplate format for PAH-solutions and elutriates of PAH-contaminated soils. Chemosphere 67:1236–1242.

62. PerkinElmer. Microplates for luminescence assays.

63. Walk CL, Bedford MR, McElroy AP. 2012. Influence of diet, phytase, and incubation time on calcium and phosphorus solubility in the gastric and small intestinal phase of an in vitro digestion assay. J Anim Sci 90:3120–3127.

64. Mollnes TE, Garred P, Bergseth G. 1988. Effect of time, temperature and anticoagulants on in vitro complement activation: consequences for collection and preservation of samples to be examined for complement activation. Clin Exp Immunol 73:484–488.

65. Björkelund H, Gedda L, Andersson K. 2011. Avoiding false negative results in specificity analysis of protein-protein interactions. J Mol Recognit 24:81–89.

66. Greig A, Stevenson K, Henderson D, Perez V, Hughes V, Pavlik I, Hines ME, Mckendrick I, Sharp JM. 1999. Epidemiological study of paratuberculosis in wild rabbits in scotland. J Clin Microbiol 37:1746–1751.

67. Beard PM, Daniels MJ, Henderson D, Pirie A, Rudge K, Buxton D, Rhind S, Greig A, Hutchings MR, McKendrick I, Stevenson K, Sharp JM. 2001. Paratuberculosis infection of nonruminant wildlife in Scotland. J Clin Microbiol 39:1517–1521.